

## EVIDENCE OF AN INITIALLY MAGNETICALLY DOMINATED OUTFLOW IN GRB 080916C

BING ZHANG<sup>1</sup> AND ASAF PE’ER<sup>2,3</sup>

<sup>1</sup> Department of Physics and Astronomy, University of Nevada, Las Vegas, NV 89154, USA

<sup>2</sup> Space Telescope Science Institute, Baltimore, MD 21218, USA

Received 2009 April 19; accepted 2009 June 17; published 2009 July 10

### ABSTRACT

The composition of gamma-ray burst (GRB) ejecta is still a mystery. The standard model invokes an initially hot “fireball” composed of baryonic matter. Here, we analyze the broadband spectra of GRB 080916C detected by the *Fermi* satellite. The featureless Band spectrum of all five epochs as well as the detections of  $\gtrsim 10$  GeV photons in this burst place a strong constraint on the prompt emission radius  $R_\gamma$ , which is typically  $\gtrsim 10^{15}$  cm, independent of the details of the emission process. The lack of detection of a thermal component as predicted by the baryonic models strongly suggests that a significant fraction of the outflow energy is initially not in the “fireball” form, but is likely in a Poynting flux entrained with the baryonic matter. The ratio between the Poynting and baryonic fluxes is at least  $\sim (15\text{--}20)$  at the photosphere radius, if the Poynting flux is not directly converted to kinetic energy below the photosphere.

*Key words:* gamma rays: bursts – gamma rays: observations – gamma rays: theory – plasmas – radiation mechanisms: non-thermal – radiation mechanisms: thermal

### 1. INTRODUCTION

In the classical model of gamma-ray bursts (GRBs), an initially hot “fireball” is composed of photons, electron/positron pairs, and a small amount of baryons (Paczyński 1986; Goodman 1986; Shemi & Piran 1990). This fireball is soon accelerated to a relativistic speed under its own thermal pressure. Due to the existence of baryons, a significant fraction of energy is converted into the kinetic energy of the ejecta (Mészáros et al. 1993; Piran et al. 1993). The rest of energy is still stored in the form of photons, which escape the system as the fireball becomes transparent at the photosphere radius (Mészáros & Rees 2000; Mészáros et al. 2002). The ejecta then coast with a relativistic speed without significant radiation until reaching a larger radius when a fraction of kinetic energy is dissipated into heat and radiation in internal shocks (Rees & Mészáros 1994). The internal shock model has the advantage of interpreting GRB variabilities, but suffers the low radiation efficiency problem (Kumar 1999; Panaitescu et al. 1999). Recently, an analysis of the prompt emission data of several GRBs suggests that the internal shock model is disfavored by the data (Kumar & McMahon 2008; Kumar & Narayan 2009). An alternative model invokes a dynamically important magnetic field. Within such a Poynting flux dominated model, the observed GRB emission is powered by dissipation of the magnetic energy within the ejecta (Usov 1994; Thompson 1994; Vlahakis & Königl 2003; Mészáros & Rees 1997; Lyutikov & Blandford 2003).

Until recently, it has been difficult to diagnose the GRB composition from observational data. The recent detection of the broadband featureless Band-function spectra as well as the very high gamma-ray emission ( $\gtrsim 10$  GeV) from GRB 080916C by the *Fermi* satellite (Abdo et al. 2009) provides a unique opportunity to diagnose the GRB composition.<sup>4</sup> Below we will use the opacity argument (Section 2) and the photosphere

argument (Section 3) to argue that the ejecta of GRB 080916C must contain a significant fraction of energy that is initially not in the “fireball” form, but in a Poynting flux entrained with baryonic matter.

### 2. MODEL INDEPENDENT EMISSION RADIUS CONSTRAINT

Both the Large Area Telescope (LAT) and the Gamma-ray Burst Monitor (GBM) onboard *Fermi* have detected GRB 080916C. The time-dependent spectral analysis reveals a series of featureless smoothly joint broken power law (“Band function;” Band et al. 1993) spectrum categorized by a peak energy  $E_p$  and two asymptotic photon spectral power-law indices  $\alpha$  and  $\beta$  (Abdo et al. 2009). These spectra cover 5–6 orders of magnitude in energy, from  $\sim 10$  keV to  $\sim (1\text{--}10)$  GeV. The highest photon energy reaches 13.2 GeV (in the time interval “d” defined in Figure 1 of Abdo et al. 2009). At a redshift  $z = 4.35 \pm 0.15$  (Greiner et al. 2009), this burst is the most energetic GRB known to date, with an isotropic gamma-ray energy  $\sim 9 \times 10^{54}$  erg.

The gamma-ray spectrum is expected to have a pair cutoff feature at large energies due to the compactness argument, i.e., the optical depth for two photon pair production ( $\gamma\gamma \rightarrow e^+e^-$ ) may reach unity above a critical cutoff energy  $E_{\text{cut}}$ . Within the internal shock model, the pair cutoff energy (or the lack of it), together with the observed variability timescale, can be used to constrain the bulk Lorentz factor  $\Gamma$  of the outflow (Baring & Harding 1997; Lithwick & Sari 2001; Abdo et al. 2009). In some models, the observed variability timescale may not reflect that of the central engine (Lyutikov & Blandford 2003; Narayan & Kumar 2009). So more generally the pair cutoff energy can be expressed as a function of two independent parameters, the bulk Lorentz factor  $\Gamma$  and the gamma-ray emission radius  $R_\gamma$  from the central engine (Gupta & Zhang 2008). For each cutoff energy  $E_{\text{cut}}$ , one can define a threshold energy  $E_{\text{id}}$  above which the photons with this energy can interact with the photons at  $E_{\text{cut}}$  to produce pairs. This threshold condition is defined by  $(E_{\text{id}}/1 \text{ MeV})(E_{\text{cut}}/1 \text{ MeV}) \gtrsim 0.25[\Gamma/(1+z)]^2$ . The expression of the pair production optical depth  $\tau_{\gamma\gamma}$  depends on the relative location between  $E_{\text{id}}$  and the Band-function break energy. For

<sup>3</sup> Riccardo Giacconi Fellow.

<sup>4</sup> An 18 GeV photon was detected earlier from GRB 941017 (Hurley et al. 1994). However, it was significantly delayed, not associated with the prompt emission. The bandpass of prompt emission observation was not wide enough to constrain the thermal emission component. Hence, it could not be applied to directly constrain the GRB emission radius and composition.

$E_p(\alpha - \beta)/(2 + \alpha) < E_{\text{id}} < E_{\text{cut}}$  (which is generally satisfied for this analysis), the optical depth of a photon with the observed energy  $E$  can be coasted into a simple form (derived from Equations (13) and (14) of Gupta & Zhang 2008, or from Equations (3–4) of Lithwick & Sari 2001 with  $\delta t$  absorbed into the expression of  $R_\gamma$  and with the cosmological correction factor  $(1 + z)$  properly taken into account)

$$\tau_{\gamma\gamma}(E) = \frac{C(\beta)\sigma_T d_z^2 f_0}{-1 - \beta} \left(\frac{E}{m_e c^2}\right)^{-1-\beta} \frac{1}{R_\gamma^2} \left(\frac{\Gamma}{1+z}\right)^{2+2\beta}, \quad (1)$$

where  $d_z = (c/H_0) \int_0^z dx / \sqrt{\Omega_\Lambda + \Omega_m(1+x)^3}$  is the comoving distance of the GRB,  $z$  is the redshift of the GRB, and  $m_e$ ,  $c$ , and  $\sigma_T$  are the fundamental constants electron mass, speed of light, and Thomson cross section, respectively. Here the energies, i.e.,  $E$  and  $m_e c^2$ , are both in units of “keV.” The parameter  $f_0$  (in units of  $\text{ph cm}^{-2} (\text{keV})^{-1-\beta}$ ) is such defined that the observed photon fluence spectrum above the break is written as  $\mathcal{N}(E) = f_0 E^\beta$ . In terms of the fitting parameters of Abdo et al. (2009),  $f_0$  can be expressed as

$$f_0 = A \cdot \Delta T \left[ \frac{E_p(\alpha - \beta)}{(2 + \alpha)} \right]^{\alpha-\beta} \exp(\beta - \alpha) (100 \text{ keV})^{-\alpha}, \quad (2)$$

where  $\Delta T$  is the (observed) time interval taken to perform the Band-function fit and  $A$  is the Band-function normalization in units of  $\text{ph cm}^{-2} \text{s}^{-1} \text{keV}^{-1}$ . Finally, the coefficient  $C(\beta)$  in Equation (1) is a function of  $\beta$ , and we adopt the approximation  $C(\beta) \simeq (7/6)(-\beta)^{-5/3}/(1 - \beta)$  (Svensson 1987) to perform the calculations.<sup>5</sup>

The lack of a spectral cutoff feature suggests  $\tau_{\gamma\gamma}(E_{\text{max}}) \leq 1$ , where  $E_{\text{max}}$  is the maximum energy of the observed photons. Using this condition, one can derive the  $\Gamma - R_\gamma$  constraints for the five time intervals (a–e) defined by (Abdo et al. 2009, using the values in their Table 1, with  $\Delta T$  defined by the time ranges listed in the table). By doing so, we have implicitly assumed that the emission location and Lorentz factor for a particular time interval  $\Delta T$  essentially remain the same. Figure 1 shows the five critical lines (solid) in the  $\Gamma - R_\gamma$  space. The allowed parameter regimes are above the lines. For all the five time intervals, the allowed emission radii are all large. This model-independent conclusion regarding a large  $R_\gamma$  is consistent with the results derived from other independent methods for other GRBs (Lyutikov 2006; Kumar & McMahon 2008; Racusin et al. 2008; Kumar & Narayan 2009; Shen & Zhang 2009).

Swift observations reveal a commonly seen steep-decay phase in the early X-ray afterglow (Tagliaferri et al. 2005), which suggests that the GRB prompt emission region is separated from the emission region of the afterglow (the external shock; Zhang et al. 2006). Within the “internal” models, the expected dissipation radius spans a wide range, from the photosphere radius (typically at  $R_{\text{ph}} \sim (10^{11} - 10^{12})$  cm) to slightly smaller than the deceleration radius ( $\sim 10^{17}$  cm). The derived large emission radius  $R_\gamma$  is inconsistent with the photosphere model (see Section 3 for details), but is consistent with that expected from the magnetic dissipation model (Lyutikov & Blandford 2003). The “internal shock” model invokes an emission radius  $R_{\text{IS}} \sim \Gamma^2 c \delta t$  (where  $\delta t$  is the variability timescale of the central

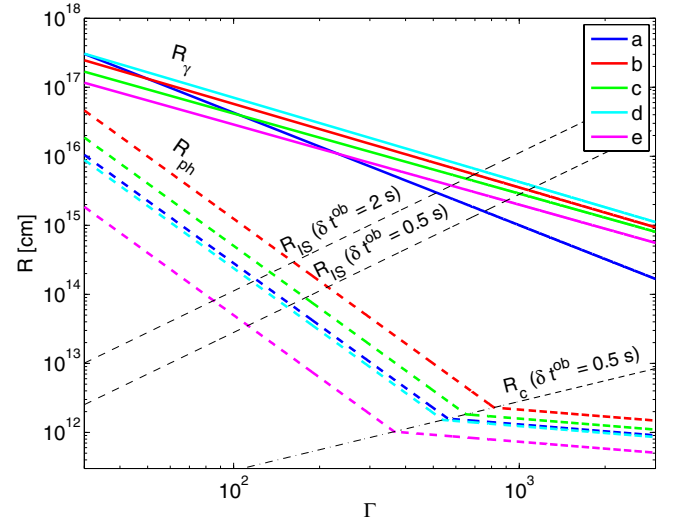


**Figure 1.**  $\Gamma - R$  diagram of GRB 080916C. The constraints on  $R_\gamma$  are displayed in color thick lines, above which are the allowed parameter spaces for each corresponding epoch. The photosphere radii  $R_{\text{ph}}$  are displayed as color dashed lines, with the same color convention. The internal shock radii  $R_{\text{IS}} = \Gamma^2 c \delta t^{\text{ob}} / (1 + z)$  for  $\delta t^{\text{ob}} = 0.5, 2$  s are the black dashed lines.

engine). The  $\Gamma - R_\gamma$  constraint of this model is plotted in Figure 1 as black dashed lines for two values of the variability timescales discussed in Abdo et al. (2009),  $\delta t = 0.5, 2$  s. The internal shock site is allowed by the data. The constrained internal shock radii are at least  $R_{\text{IS}} \sim 10^{15} - 10^{16}$  cm for the five epochs. The required Lorentz factors are at least 500–1000 (see Figure 1). However, there are further constraints on this model, as discussed below.

### 3. CONSTRAINTS FROM THE PHOTOSPHERIC (THERMAL) EMISSION

Besides the energy dissipation region (internal shock or magnetic dissipation site), the fireball “photosphere,” at which the fireball becomes transparent during the expansion, is another emission site of GRBs (Mészáros & Rees 2000; Rees & Mészáros 2005; Thompson et al. 2007; Ghisellini et al. 2007; Lazzati et al. 2009). The photosphere radius  $R_{\text{ph}}$  is defined by the electron scattering optical depth  $\tau'_{\gamma e} = n' \sigma_T \Delta' = 1$ , where  $n'$  and  $\Delta'$  are the electron number density and width of the ejecta shell in the rest frame comoving with the ejecta. Below we will assume a pure baryonic flow (as expected in the fireball model) to derive the expected photosphere spectra. For a continuous baryonic wind (which is suitable to describe GRB 080916C given the smooth light curves reported in Figure 1 of Abdo et al. 2009) with a total wind luminosity  $L_w$ , the photosphere radius can be written as (Mészáros & Rees 2000; Pe'er 2008)  $R_{\text{ph}} \simeq (L_w \sigma_T R_0^2 / 8\pi m_p c^3 \eta)^{1/3}$  for  $R_{\text{ph}} < R_c$  and  $R_{\text{ph}} \simeq L_w \sigma_T / 8\pi m_p c^3 \Gamma^2 \eta$  for  $R_{\text{ph}} > R_c$ . Here,  $m_p$  is the proton mass,  $\eta = L_w / \dot{M} c^2$  is the dimensionless entropy of the baryonic flow, and  $R_c \sim R_0 \cdot \min(\eta, \eta_*)$  is the radius at which the ejecta wind reaches the “coasting” phase. The critical dimensionless entropy is  $\eta_* = (L_w \sigma_T / 8\pi m_p c^3 R_0)^{1/4}$ , and  $R_0 = c \delta t$  is the radius where the ejecta is emitted from the central engine. The coasting Lorentz factor is  $\Gamma = \eta$  for  $R_{\text{ph}} > R_c$  and  $\Gamma = \eta_*$  for  $R_{\text{ph}} \leq R_c$ . The photosphere radii for the five epochs of GRB 080916C are presented in Figure 1 by the color dashed lines.

It has been suggested that the observed  $E_p$  of GRBs may be the thermal peak of the photosphere emission (Rees & Mészáros 2005; Thompson et al. 2007), and that the Comptonization of the

<sup>5</sup> Gupta & Zhang (2008) take  $C(\beta) = 3/8(1 - \beta)$ , while Lithwick & Sari (2001) take  $C(\beta) = 11/180$ . For a typical value  $\beta = -2$ , the  $C(\beta)$  values of Svensson (1987) and Gupta & Zhang (2008) are consistent with each other, but that of Lithwick & Sari (2001) is smaller by a factor of  $\sim 2$ .

thermal emission may lead to a nonthermal spectrum above  $E_p$  (Pe'er et al. 2005, 2006). However, for GRB 080916C, Figure 1 suggests that the observed gamma-ray emission is *not* from the photosphere, since  $R_\gamma \gg R_{\text{ph}}$ . Under the high-compactness condition, a second photosphere may be formed (Mészáros et al. 2002; Kobayashi et al. 2002; Pe'er & Waxman 2004), but its radius is also much smaller than  $R_\gamma$  inferred from the data. Another suggestion is that the observed GRB spectra are the superposition of a thermal component (photosphere) that defines  $E_p$  and a nonthermal power-law component (Ryde 2005; Ryde & Pe'er 2008). This model is based on the data in a relatively narrow spectral range of BATSE, and when extrapolated to high energies, would violate the observed featureless Band function significantly. The theoretically expected thermal peak energy  $\approx 50$  keV (see below) is well below the observed  $E_p$  in the five epochs discussed by Abdo et al. (2009). Clearly, this model by itself is insufficient to interpret the data of this burst.

The initial wind luminosity  $L_w$  of the fireball is at least the observed gamma-ray luminosity  $L_\gamma$  (assuming radiation efficiency 100%), i.e.,  $L_w \geq L_\gamma$ . Such an outflow, during the expansion, must have released a residual thermal emission at the transparent (photosphere) radius. The luminosity of this thermal component is high, and can be written as (Mészáros & Rees 2000)

$$L_{\text{th}} = \begin{cases} L_w, & \eta > \eta_*, R_{\text{ph}} < R_c, \\ L_w(\eta/\eta_*)^{8/3}, & \eta < \eta_*, R_{\text{ph}} > R_c. \end{cases} \quad (3)$$

The expected temperature of the blackbody component emerging from the photosphere is thus  $T_{\text{ph}}^{\text{ob}} = (L_w/4\pi R_0^2 c a)^{1/4}(1+z)^{-1}$  for  $R_{\text{ph}} < R_c$  and  $T_{\text{ph}}^{\text{ob}} = (L_w/4\pi R_0^2 c a)^{1/4}(R_{\text{ph}}/R_c)^{-2/3}(1+z)^{-1}$  for  $R_{\text{ph}} > R_c$ , respectively, where  $a$  is Stefan–Boltzmann’s constant.

Assuming a blackbody spectrum (other modified spectral shapes would not change the conclusion), we plot in Figure 2 the *lower limit* of the expected photosphere spectrum for the internal shock model in the baryon-dominated outflow (by taking  $L_w = L_\gamma$ ) and compare it with the observations. For clarity, only the predictions for the epoch (b) are plotted (red thick-dashed curve). This plot corresponds to  $\eta \geq \eta_* = 850$ , hence  $L_{\text{th}} = L_w$ ,  $R_{\text{ph}} \simeq R_c$  and  $T_{\text{ph}}^{\text{ob}} = T_{\text{ph,max}}^{\text{ob}} = 50$  keV. It is apparent that such a component strongly violates the observational data, which is a featureless Band function.

One can further argue that the baryonic model in general does not work. In Figure 2, we present the predicted lower limits of the photosphere spectrum for two additional (more conservative) temperatures  $T_{\text{ph}}^{\text{ob}} = 10, 1$  keV. These correspond to either a coasting Lorentz factor  $\eta = 470, 200$  (for the same  $\delta t^{\text{ob}}$ ), or a central engine variability timescale much longer than what is observed (for the same  $\eta$ ), which may be relevant to a fireball emerging from a stellar envelope in the collapsar model. These models give a much larger  $R_{\text{ph}}$ , and hence, a much lower  $T_{\text{ph}}^{\text{ob}}$ . Since  $\delta t^{\text{ob}} = 0.5$  s has been observed (Abdo et al. 2009), the models that invoke a longer central engine variability timescale require the unconventional assumption that the observed variability timescale is not that of the central engine (Narayan & Kumar 2009). Nonetheless, the predicted thermal spectra of these cases (red, thin-dashed curves) also strongly violate the observational constraints.

This analysis strongly suggests that the initial wind luminosity was not stored in the “fireball” form at the base of the central engine. Since there is no other known source of energy that can be entrained in the ejecta, we identify the missing lumi-

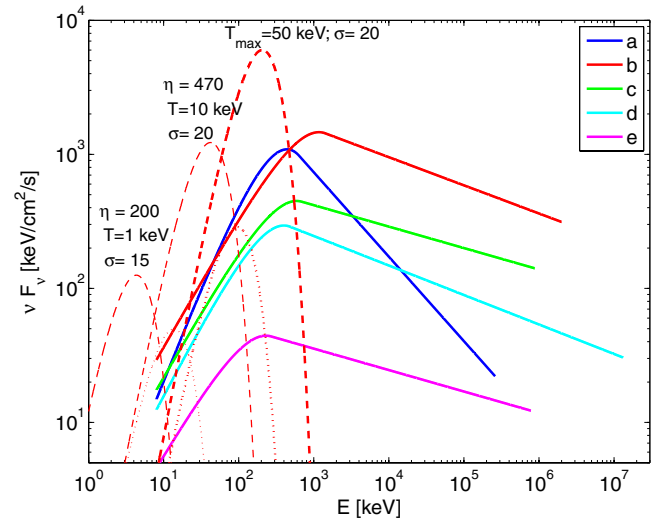


**Figure 2.** Observed Band-function spectra for the five epochs (Abdo et al. 2009) (color solid) and the predicted lower limits of the photosphere spectra (red dashed) for different parameters for the epoch (b) within the framework of the baryonic fireball models. Red, thick-dashed curve: the internal shock model with  $\delta t^{\text{ob}} = 0.5$  s, corresponding to  $T_{\text{ph}}^{\text{ob}} = 50$  keV; red, thin-dashed curves: for  $T_{\text{ph}}^{\text{ob}} = 10, 1$  keV. The suppressed photosphere spectra are plotted by red, dotted curves, with the required  $\sigma$  values marked.

nosity as the Poynting flux luminosity, which is not observable before strong magnetic dissipation occurs at a much larger radius. It has been suggested (Zhang & Mészáros 2002; Daigne & Mochkovitch 2002) that the photosphere thermal component can be much dimmer if the outflow is Poynting flux dominated. In order to hide the bright thermal component, one can pose a lower limit on the ratio between the Poynting flux and the baryonic flux,  $\sigma \equiv L_P/L_b$ . Following Zhang & Mészáros (2002), we define  $L_w = L_b + L_P = (1 + \sigma)L_b$ . Assuming no dissipation of the Poynting flux below  $R_{\text{ph}}$ , the above photosphere derivations can be modified by replacing  $L_w$  by  $L_w/(1 + \sigma)$ . One can then derive the required minimum  $\sigma$  value that can “hide” the photosphere thermal component. For the specific internal shock model required by the variability timescale (the red thick-dashed curve), one requires at least  $\sigma \simeq 20$  at the photosphere to make the photosphere emission unobservable (red thick-dotted curve in Figure 2). At such a high- $\sigma$  shocks are very weak and cannot power the bright gamma-ray emission (Zhang & Kobayashi 2005), so unless  $\sigma$  can reduce significantly from the photosphere to the internal shock radius (e.g., Spruit et al. 2001) but without generating a dominant emission component in the observed spectrum, the internal shock model is not a viable mechanism to interpret this burst.<sup>6</sup> For the other two unconventional cases, similar minimum values of  $\sigma = 15$ –20 at photosphere are required in order to obtain consistency with the observed spectra. We can therefore conclude that the ejecta of GRB 080916C cannot be a pure “fireball,” but must store a significant fraction of energy initially in a Poynting flux.

#### 4. SUMMARY AND DISCUSSION

In this Letter, we show that the observed featureless Band-function broadband spectra of GRB 080916C observed by

<sup>6</sup> Another possibility would be that the Poynting flux is converted to kinetic energy directly without magnetic dissipation during the acceleration phase (e.g., Vlahakis & Königl 2003). The photosphere brightness of this model is not studied in detail.

the *Fermi* satellite (Abdo et al. 2009) pose two interesting constraints on the GRB prompt emission mechanism. First, the detection of high energy,  $\gtrsim 10$  GeV, photons places a strong model-independent  $\Gamma - R_\gamma$  constraint on the GRB ejecta (Figure 1), which precludes the photosphere ( $R_{\text{ph}} \ll R_\gamma$ ) as the emission site. Second, the nondetection of a bright thermal component expected from the baryonic models puts a strong constraint on the composition of the fireball: the flow should be dominated by a Poynting flux component with a minimum  $\sigma \approx 15\text{--}20$  at the photosphere in order to account for the observed spectra (Figure 2), as long as the Poynting flux energy is not directly converted to the kinetic energy of the flow below the photosphere.

Within such a picture, the observed bright gamma-ray emission may be powered by dissipation of the Poynting flux energy within the outflow. A Poynting flux dominated flow favors synchrotron radiation as the emission mechanism of the observed gamma rays. This is consistent with independent modeling of the burst (Wang et al. 2009). It also suggests a weak synchrotron self-Compton component, which is not observed from the data. This model requires that the GRB central engine launches a collimated magnetic bubble from the central engine (black hole or millisecond magnetar), which propagates through the stellar envelope without reducing the  $\sigma$  value significantly (Wheeler et al. 2000). After escaping the star, the ejecta is quickly accelerated under its own magnetic pressure (Mizuno et al. 2009). At the radius where photons become transparent (photosphere), the bulk of the wind energy is not in the thermal form. The  $\sigma$  value may reduce above photosphere. However, in order to have internal shocks, the magnetic energy needs to be “quietly” dissipated below the internal shock radius without significant emission. More naturally, the magnetic field may be globally dissipated in a cataclysmic manner to power the observed emission. This model does not demand a high- $\sigma$  at the deceleration radius, since  $\sigma$  of the flow would decrease significantly in the prompt emission region due to intense magnetic dissipation. In any case, the  $\sigma$  value at the deceleration radius can be of order unity or higher, which gives a weak or moderately bright reverse shock emission component (Zhang & Kobayashi 2005; Mimica et al. 2009).

This analysis applies to GRB 080916C. Similar analyses can be carried out for more bursts co-detected by *Fermi* LAT/GBM in the future to determine whether other GRB outflows are also magnetically dominated.

We thank F. Ryde for discussion on the *Fermi* data, M. Baring, Z. G. Dai, Y. Z. Fan, G. Ghisellini, D. Giannios, P. Kumar, E. P. Liang, P. Mészáros, S. Nagataki, K.-I. Nishikawa, C. Thompson, K. Toma, N. Vlahakis, X. Y. Wang, X. F. Wu, and

H. Yan for discussions/comments. B.Z. acknowledges NASA NNG05GB67G, NNX08AN24G, and NNX08AE57A, and A.P. acknowledges the Riccardo Giacconi Fellowship at the Space Telescope Science Institute for supports.

## REFERENCES

- Abdo, A. A., et al. 2009, *Science*, **323**, 1688  
 Band, D., et al. 1993, *ApJ*, **413**, 281  
 Baring, M. G., & Harding, A. K. 1997, *ApJ*, **491**, 663  
 Daigne, F., & Mochkovitch, R. 2002, *MNRAS*, **336**, 1271  
 Ghisellini, G., et al. 2007, *MNRAS*, **382**, L72  
 Goodman, J. 1986, *ApJ*, **308**, L47  
 Greiner, J., et al. 2009, *A&A*, **498**, 89  
 Gupta, N., & Zhang, B. 2008, *MNRAS*, **384**, L11  
 Hurley, K., et al. 1994, *Nature*, **372**, 652  
 Kobayashi, S., Ryde, F., & MacFadyen, A. 2002, *ApJ*, **577**, 302  
 Kumar, P. 1999, *ApJ*, **523**, L113  
 Kumar, P., & McMahon, E. 2008, *MNRAS*, **384**, 33  
 Kumar, P., & Narayan, R. 2009, *MNRAS*, **395**, 472  
 Lazzati, D., Morsony, B. J., & Begelman, M. 2009, *ApJ*, in press (arXiv:0904.2779)  
 Lithwick, Y., & Sari, R. 2001, *ApJ*, **555**, 540  
 Lyutikov, M. 2006, *MNRAS*, **369**, L5  
 Lyutikov, M., & Blandford, R. 2003, arXiv:astro-ph/0312347  
 Mészáros, P., Laguna, P., & Rees, M. J. 1993, *ApJ*, **415**, 181  
 Mészáros, P., Ramirez-Ruiz, E., Rees, M. J., & Zhang, B. 2002, *ApJ*, **578**, 812  
 Mészáros, P., & Rees, M. J. 1997, *ApJ*, **482**, L29  
 Mészáros, P., & Rees, M. J. 2000, *ApJ*, **530**, 292  
 Mimica, P., Giannios, D., & Aloy, M. A. 2009, *A&A*, **494**, 879  
 Mizuno, Y., et al. 2009, *ApJ*, **690**, L47  
 Narayan, R., & Kumar, P. 2009, *MNRAS*, **394**, L117  
 Paczyński, B. 1986, *ApJ*, **308**, L43  
 Panaitescu, A., Spada, M., & Mészáros, P. 1999, *ApJ*, **522**, L105  
 Pe'er, A. 2008, *ApJ*, **682**, 463  
 Pe'er, A., Mészáros, P., & Rees, M. J. 2005, *ApJ*, **635**, 476  
 Pe'er, A., Mészáros, P., & Rees, M. J. 2006, *ApJ*, **642**, 995  
 Pe'er, A., & Waxman, E. 2004, *ApJ*, **613**, 448  
 Piran, T., Shemi, A., & Narayan, R. 1993, *MNRAS*, **263**, 861  
 Racusin, J. L., et al. 2008, *Nature*, **455**, 183  
 Rees, M. J., & Mészáros, P. 1994, *ApJ*, **430**, L93  
 Rees, M. J., & Mészáros, P. 2005, *ApJ*, **628**, 847  
 Ryde, F. 2005, *ApJ*, **625**, L95  
 Ryde, F., & Pe'er, A. 2008, arXiv:0811.4135  
 Shemi, A., & Piran, T. 1990, *ApJ*, **365**, L55  
 Shen, R.-F., & Zhang, B. 2009, *MNRAS*, in press (arXiv:0906.2597)  
 Spruit, H. C., Daigne, F., & Drenkhahn, G. 2001, *A&A*, **369**, 694  
 Svensson, R. 1987, *MNRAS*, **227**, 403  
 Tagliaferri, G., et al. 2005, *Nature*, **436**, 985  
 Thompson, C. 1994, *MNRAS*, **270**, 480  
 Thompson, C., Mészáros, P., & Rees, M. J. 2007, *ApJ*, **666**, 1012  
 Usov, V. V. 1994, *MNRAS*, **267**, 1035  
 Vlahakis, N., & Königl, A. 2003, *ApJ*, **596**, 1104  
 Wang, X.-Y., Li, Z., Dai, Z.-G., & Mészáros, P. 2009, *ApJ*, **698**, L98  
 Wheeler, J. C., Yi, I., Höflich, P., & Wang, L. 2000, *ApJ*, **537**, 810  
 Zhang, B., & Kobayashi, S. 2005, *ApJ*, **628**, 315  
 Zhang, B., & Mészáros, P. 2002, *ApJ*, **581**, 1236  
 Zhang, B., et al. 2006, *ApJ*, **642**, 354